

See discussions, stats, and author profiles for this publication at: <https://www.researchgate.net/publication/337953533>

The great isotopic dichotomy of the early Solar System

Article in *Nature Astronomy* · December 2019

DOI: 10.1038/s41550-019-0959-9

CITATIONS

9

READS

397

3 authors, including:



Thomas S. Kruijer

Lawrence Livermore National Laboratory

67 PUBLICATIONS 1,030 CITATIONS

[SEE PROFILE](#)



Lars E. Borg

Lawrence Livermore National Laboratory

185 PUBLICATIONS 4,683 CITATIONS

[SEE PROFILE](#)

Some of the authors of this publication are also working on these related projects:



Petrology of Mars [View project](#)



Modelling of accretion and differentiation of the Proto-Earth and its building blocks [View project](#)

The great isotopic dichotomy of the early Solar System

Thomas S. Kruijer^{1*}, Thorsten Kleine² and Lars E. Borg¹

The isotopic composition of meteorites and terrestrial planets holds important clues about the earliest history of the Solar System and the processes of planet formation. Recent work has shown that meteorites exhibit a fundamental isotopic dichotomy between non-carbonaceous (NC) and carbonaceous (CC) groups, which most likely represent material from the inner and outer Solar System, respectively. Here we review the isotopic evidence for this NC–CC dichotomy, discuss its origin and highlight the far-reaching implications for the dynamics of the solar protoplanetary disk. The NC–CC dichotomy combined with the chronology of meteorite parent-body accretion mandate an early and prolonged spatial separation of inner (NC) and outer (CC) disk reservoirs, lasting between ~1 and ~4 Myr after Solar System formation. This is most easily reconciled with the early and rapid growth of Jupiter’s core, inhibiting substantial exchange of material from inside and outside its orbit. The growth and migration of Jupiter also led to the later implantation of CC bodies into the inner Solar System and, therefore, can explain the co-occurrence of NC and CC bodies in the asteroid belt, and the delivery of volatile and water-rich CC bodies to the terrestrial planets.

The Solar System formed by the gravitational collapse of a molecular cloud core, which resulted in the formation of a circumsolar disk of gas and dust (sometimes called the ‘solar nebula’). This disk was ultimately transformed into a planetary system consisting of a single central star, the Sun, surrounded by four terrestrial planets in the inner Solar System, four giant planets in the outer Solar System beyond the ‘snow line’, and a multitude of smaller bodies, including asteroids, moons, dwarf planets and comets. To understand how the Solar System evolved towards its present-day configuration, the events and processes occurring during the earliest stages of Solar System history must be reconstructed at a very high temporal and spatial resolution. Although astronomical observations¹ and dynamical modelling² provide fundamental insights into the structure and dynamics of protoplanetary disks, and the processes of planetary accretion, the study of meteorites allows the reconstruction of the Solar System’s earliest history with unprecedented resolution in time and space. Recent analytical advances in the precision of isotope ratio measurements make it possible not only to date meteorites at submillion-year precision^{3–5} (see Box 1) but also to identify distinct nucleosynthetic isotopic signatures. This allows genetic links between planetary materials to be determined and helps constrain the area of the disk a given meteorite originated from^{6–8}.

Most meteorites derive from asteroids that are at present located in the main asteroid belt between Mars and Jupiter (at ~2.0–3.3 au), and have traditionally been viewed as samples from bodies that formed where they are found today. However, recently, this perspective has changed dramatically with the discovery of a fundamental genetic dichotomy observed in the nucleosynthetic isotope signatures of non-carbonaceous (NC) and carbonaceous (CC) meteorites^{6,8,9}. This discovery, combined with the establishment of a precise chronology for the accretion of meteorite parent bodies, has enabled the integration of meteoritic constraints into large-scale models of disk evolution and planet formation.

The non-carbonaceous–carbonaceous meteorite dichotomy

Nucleosynthetic isotope anomalies arise from the heterogeneous distribution of presolar phases, and ultimately reflect that the Solar System incorporated material from different stellar sources. As evident from analyses of presolar grains contained in primitive meteorites, the Solar System’s molecular cloud comprised materials with strongly variable isotopic compositions¹⁰. Although processes within the Solar System’s parental molecular cloud and/or the circumsolar disk homogenized these materials relatively well, small heterogeneities exist that have been sampled at the scale of meteorite components, bulk meteorites and planets¹¹. Nucleosynthetic isotope anomalies have been identified for many elements, but here we focus on those that are most relevant for the definition of the NC–CC dichotomy and, hence, provide the most detailed insights into the dynamics of the early Solar System.

Meteorites exhibit notable isotope anomalies for elements such as O, Cr and Ti (note that the O isotope anomalies are not nucleosynthetic in origin, but nevertheless are indicative of spatial or temporal changes of solid material in the disk¹²). As such, it is no surprise that the NC–CC dichotomy was first recognized based on isotope anomalies for these three elements⁸. The dichotomy is most clearly observed when different isotope anomalies (for example, ⁵⁴Cr versus ⁵⁰Ti) are plotted against each other (Fig. 1). In spite of isotope variations among bulk meteorites within each reservoir, there is a clear ‘gap’ between the NC and CC reservoirs, indicating that there has not been substantial mixing of NC and CC materials during the formation of meteorites. Subsequent studies demonstrated that the NC–CC dichotomy extends to other elements, such as Ni (refs. ^{13,14}; Fig. 1d) and Mo (refs. ^{6,9,15,16}; Fig. 2a). Molybdenum is especially useful in identifying the NC–CC dichotomy because it allows anomalies of distinct origins to be distinguished and because, unlike Ti and Cr, the isotopic composition of Mo can be analysed in essentially all meteorites. Specifically, the heterogeneous distribution of carriers enriched in nuclides produced in the slow neutron capture process (s-process)

¹Nuclear and Chemical Sciences Division, Lawrence Livermore National Laboratory, Livermore, CA, USA. ²Institut für Planetologie, University of Münster, Münster, Germany. *e-mail: kruijer1@llnl.gov

Box 1 | Dating meteorites using isotope chronometers

Radioactive decay systems used for dating meteorites can be subdivided into long-lived and short-lived chronometers. Of these, the ^{207}Pb – ^{206}Pb isotope system, which is based on the decay of long-lived ^{235}U and ^{238}U , can provide very precise absolute ages for meteorites and their components^{3,19,74}, as long as they are corrected for variable $^{235}\text{U}/^{238}\text{U}$ in early Solar System materials⁹⁰. Short-lived radionuclides are isotopes that existed at the beginning of Solar System history but that have since decayed. Hence, their presence in the early Solar System can be detected only by studying the isotopic composition of their daughter isotopes. Important examples of short-lived chronometers that are highly relevant for early Solar System chronology include the ^{26}Al – ^{26}Mg (half-life: ~ 0.7 Myr) and ^{182}Hf – ^{182}W (half-life: ~ 9 Myr) systems.

For establishing a precise chronology of the early Solar System, it is useful to define a common reference point, which is typically defined by the formation of the oldest dated solids, known as Ca–Al-rich inclusions (CAIs). These refractory inclusions are thought to have formed close to the young Sun⁹¹, and were subsequently transported outwards to the accretion region of carbonaceous chondrites^{57,58}. The Pb–Pb age of CAIs of $4,567.2 \pm 0.2$ Myr is generally considered to effectively date the start of Solar System history, or ‘time zero’ in cosmochemistry^{3,19}. CAIs also have the highest initial $^{26}\text{Al}/^{27}\text{Al}$ and $^{182}\text{Hf}/^{180}\text{Hf}$ ratios of any meteoritic material^{30,54,55,92}, making them pivotal reference points for the Solar System’s initial compositions of various decay systems. However, there are also CAIs that lack evidence for live ^{26}Al , and these CAIs are thought to have formed slightly earlier than the more common ‘normal’ CAIs, before injection of ^{26}Al into the Solar System^{93–95}. Nevertheless, in early Solar System chronology, ages are generally given as the time elapsed since formation of ‘normal’ CAIs dated at $4,567.2 \pm 0.2$ Myr.

The Al–Mg system provides very precise relative isochron ages for meteorite components such as CAIs^{54,55} and chondrules^{5,36,38}. These ages are chronologically meaningful only when ^{26}Al was distributed homogeneously throughout the Solar System, which is debated^{27–30}.

The Hf–W system is widely used to date planetary core formation, both on meteorite parent bodies and on larger bodies like the Earth^{83,84}. This is because both Hf and W are refractory elements but have different geochemical affinities during metal–silicate separation. As W is moderately siderophile and Hf strongly lithophile, core–mantle differentiation results in high Hf/W in the mantle, and Hf/W of essentially zero in the core. Hence, the Hf–W system can be used to provide model ages for the timing of core formation in planetary bodies that accreted during the earliest stages of Solar System history (that is, within the effective lifetime of ^{182}Hf).

of stellar nucleosynthesis and the rapid neutron capture process (r-process) results in different patterns of Mo isotope anomalies within individual samples¹⁷. These variable nucleosynthetic components are most clearly seen in a plot of $\epsilon^{95}\text{Mo}$ versus $\epsilon^{94}\text{Mo}$ (the parts-per-10,000 deviations of the $^{95}\text{Mo}/^{96}\text{Mo}$ and $^{94}\text{Mo}/^{96}\text{Mo}$ ratios from terrestrial standard values), where NC and CC meteorites define two separate and parallel s-process mixing lines with a resolved offset between the two lines (Fig. 2a). This offset reflects an approximately homogeneous enrichment in r-process nuclides in the CC over the NC reservoir^{6,18} and possibly also an enrichment in p-nuclei^{15,16}, which are produced by proton capture and/or other nucleosynthetic processes. The fact that Mo can be analysed in a wide range of sample types leads to the realization that the NC–CC dichotomy is a fundamental and ubiquitous characteristic of the entire meteorite record.

As will be discussed in more detail below, the NC–CC dichotomy most likely reflects the separation of the early Solar System into an inner and outer disk separated by Jupiter. As carbonaceous chondrites are commonly assumed to have accreted at greater heliocentric distances than ordinary and enstatite chondrites, and because Earth and Mars plot within the NC field (Fig. 1), the NC reservoir represents the inner and the CC reservoir the outer Solar System⁸.

Meteorite chronology in light of the NC–CC dichotomy

Utilizing the NC–CC dichotomy of meteorites to understand the evolution of the early Solar System and determining whether the dichotomy reflects temporal and/or spatial changes in the isotopic composition of the disk requires knowledge of the timescales of meteorite parent-body accretion. However, parent-body accretion cannot be dated directly, but must be inferred either by dating the formation of a specific component (for example, chondrules) that is closely linked in time to the accretion of their parent body, or alternatively, by dating a specific chemical differentiation process (for example, core formation), which can be linked to the time of parent-body accretion via thermal modelling. Rather than providing a comprehensive summary of the chronology of meteorites, here we focus on those ages that provide the most precise constraints on the accretion timescales of NC and CC meteorite parent bodies. Below we distinguish between the accretion ages for the parent bodies of differentiated meteorites (‘Differentiated meteorites and the first planetesimals’) and of chondrite parent bodies (‘Late’ accretion of chondrite parent bodies’). Note that all ages are given relative to the start of Solar System history $4,567.2 \pm 0.2$ Myr ago^{3,19} as defined by the ages of Ca–Al-rich inclusions (CAIs; see Box 1).

Differentiated meteorites and the first planetesimals.

Differentiated meteorites include samples from the metallic cores (that is, iron meteorites) as well as silicate mantles and crusts (for example, angrites, eucrites, ureilites) of differentiated asteroids. Collectively, the meteorite ages demonstrate that planetesimal differentiation occurred within the first few million years after CAI formation²⁰, consistent with heating driven mainly by ^{26}Al decay²¹. The most direct evidence for early planetesimal differentiation comes from the Hf–W chronometry of ‘magmatic’ iron meteorites, which are thought to sample the cores of differentiated protoplanets²². The Hf–W model ages of core formation (Box 1) are between ~ 0.3 and ~ 1.8 Myr for NC irons, and between ~ 2.2 and ~ 2.8 Myr for CC irons^{4,9} (Fig. 3b). Combining the Hf–W ages with thermal modelling of bodies internally heated by ^{26}Al decay demonstrates that NC iron meteorite parent bodies accreted less than 0.5 Myr after CAI formation, whereas CC iron meteorite parent bodies accreted less than 1 Myr after CAI formation^{4,9} (Fig. 4). Iron meteorite parent bodies, therefore, are among the first planetesimals formed in the Solar System. A corollary of this observation is that rapid formation of differentiated planetesimals (that is, of iron meteorite parent bodies) was possible not only in the innermost terrestrial planet region²³ but also in the outer disk (that is, the CC reservoir).

Accretion timescales can in principle also be inferred for the parent bodies of differentiated achondrites (for example, angrites, eucrites, ureilites). However, these accretion ages are less well constrained, because there are additional parent-to-daughter (for example, Hf–W or Al–Mg) fractionation events in the silicate mantles subsequent to core formation. The isotopic compositions of these samples, therefore, reflect more than one differentiation event, making the model ages for core formation more uncertain. Nevertheless, there is general agreement that the angrite and eucrite parent bodies accreted well within the first ~ 1 – 2 Myr of the Solar System^{24–26}, and thus as early as the iron meteorite parent bodies. However, extremely early accretion ages reported for the angrite and ureilite parent bodies^{27,28} hinge on the contested^{29,30} assumption

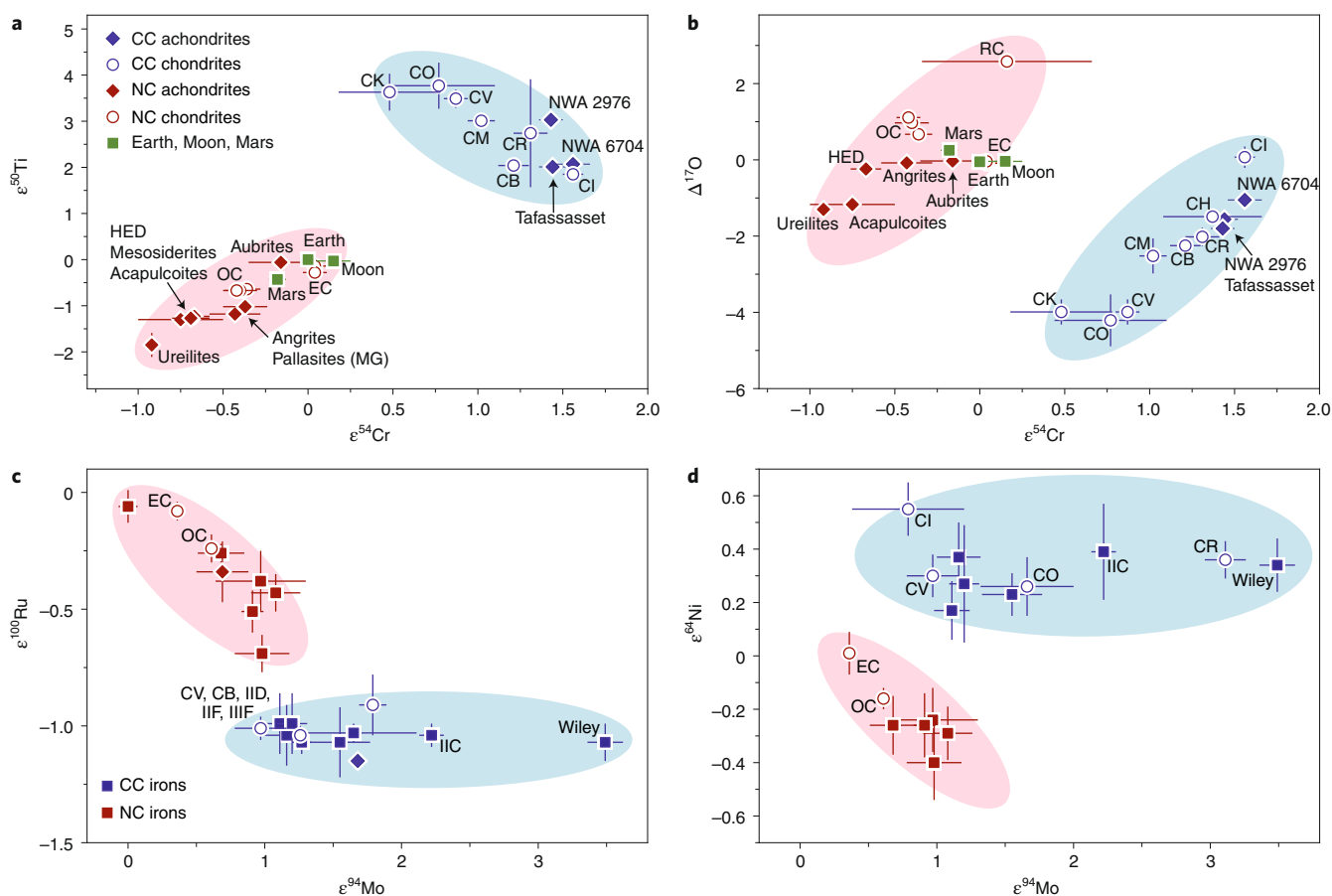


Fig. 1 | NC–CC meteorite dichotomy inferred from isotopic signatures of bulk meteorites. a–d, $\epsilon^{50}\text{Ti}$ versus $\epsilon^{54}\text{Cr}$ (**a**), $\Delta^{17}\text{O}$ versus $\epsilon^{54}\text{Cr}$ (**b**), $\epsilon^{100}\text{Ru}$ versus $\epsilon^{94}\text{Mo}$ (**c**), $\epsilon^{64}\text{Ni}$ versus $\epsilon^{94}\text{Mo}$ (**d**). Note that 1 ϵ -unit represents the 0.01% deviation (and 1 δ -unit the 0.1% deviation) in the isotopic ratio of a sample relative to terrestrial rock standards. Mass-independent O isotope variations are expressed in $\Delta^{17}\text{O}$ ($\Delta^{17}\text{O} \equiv \delta^{17}\text{O} - 0.52\delta^{18}\text{O}$, where 0.52 is the slope of mass-dependent mass fractionation). Note that $\Delta^{17}\text{O}$ variations are not nucleosynthetic in origin, but probably reflect photochemical processes in the molecular cloud or the solar nebula¹². Errors bars denote external uncertainties (2σ) reported in respective studies. OC, ordinary chondrites; EC, enstatite chondrites; RC, rumuruti chondrites; HED, howardites, eucrites, diogenites; MG, Main Group. The isotopic data plotted here are summarized and tabulated in refs. ^{18,56}.

of a heterogeneous distribution of ^{26}Al in the Solar System, and the ureilite parent body in particular may have accreted slightly later than the parent bodies of other differentiated objects³¹. Regardless of these uncertainties, the chronology of differentiated achondrites indicates that these meteorites, like the irons, derive from an early generation of planetesimals.

‘Late’ accretion of chondrite parent bodies. Chondrites are thought to derive from asteroids that never melted and, therefore, preserved components that formed before their accretion. Of these, millimetre-sized igneous spherules known as chondrules are not only the most dominant but also the most extensively dated component. Different mechanisms for chondrule formation have been proposed, but no consensus about their formation process has yet been reached³². Chondrules may have formed by melting of dust aggregates in the solar protoplanetary disk, which might have facilitated the accumulation of dust into planetesimals^{33,34}. They may also have formed during protoplanetary impacts and would then merely be a by-product of planet formation³⁵. Regardless of their exact formation process, chondrules formed before their assembly into chondrite parent bodies, and so dating chondrule formation constrains the timescale of chondrite parent-body accretion.

Ages for chondrules are typically obtained either by pooling multiple chondrules (Pb–Pb, Hf–W) or by dating single chondrules (Al–Mg, Pb–Pb). Perhaps the most stringent constraint comes from Al–Mg chronometry of individual chondrules from the least altered chondrites, revealing clear age peaks at ~ 2 – 3 Myr (for chondrules from ordinary, CV and CO chondrites) and at ~ 3.7 Myr (CR chondrites) after CAI formation^{5,36–39} (Fig. 3a). These ages are in excellent agreement with Hf–W^{29,34} and Pb–Pb^{40–43} ages of pooled chondrule separates from CV and CR chondrites, indicating that the vast majority of chondrules formed between ~ 2 and ~ 4 Myr after CAI formation (Fig. 3a). Moreover, chondrules from a given chondrite group formed in a narrow time span of <1 Myr, suggesting that they rapidly accreted into their parent bodies. The youngest chondrule ages of ~ 4 – 5 Myr are obtained for CB chondrites^{44,45}, but their formation process was probably different from that of other, more common chondrules^{45,46}.

Given this consistent picture of chondrule chronology, it is surprising that Pb–Pb ages for some individual chondrules from a given chondrite group display a spread in ages from ~ 0 to 4 Myr, whereas Al–Mg ages remain relatively constant^{3,47,48}. One possibility to account for the disparity between Pb–Pb and Al–Mg ages for single chondrules is that ^{26}Al was heterogeneously distributed among the chondrule precursors, and that variations in ^{26}Al abundances,

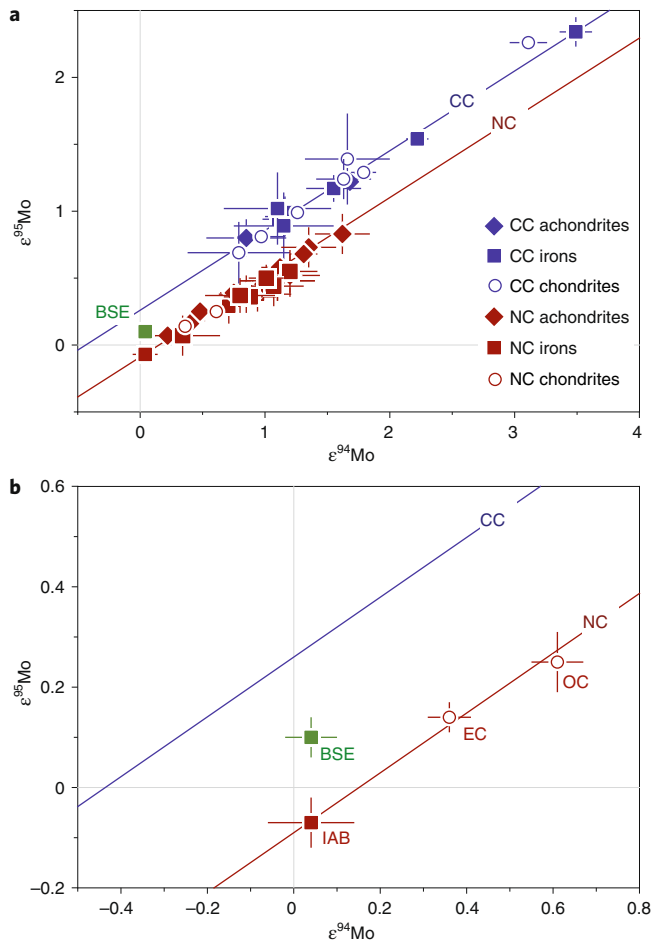


Fig. 2 | Molybdenum isotope dichotomy of meteorites. a, $\epsilon^{95}\text{Mo}$ versus $\epsilon^{94}\text{Mo}$ data for bulk meteorites. NC (red) and CC (blue) meteorites define two parallel s-process mixing lines with identical slopes, but distinct intercept values^{6,918}. The offset between the two lines reflects an approximately uniform r-process excess in the CC reservoir relative to the NC reservoir. **b**, Zoomed-in version of **a** illustrating that the BSE plots between the NC and CC lines. Plotted NC and CC lines are based on regression results reported in ref. ¹⁸. Error bars denote external uncertainties reported in respective studies (2σ). A summary of the Mo isotopic data shown in the figure is also given in ref. ¹⁸. Abbreviations as given in main text and Fig. 1; group IAB non-magmatic iron meteorites are denoted 'IAB'. Figure reproduced with permission from ref. ¹⁸, Springer Nature Ltd.

therefore, have no chronological meaning^{47,48}. This, however, is not easily reconciled with the good agreement of Hf–W and Al–Mg ages for meteorites^{29,30}, and with the good agreement between Al–Mg, Hf–W and Pb–Pb ages for pooled chondrule separates (Fig. 3a). A heterogeneous ²⁶Al distribution would also lead to an apparent range in Al–Mg chondrule ages, instead of a single well-defined age peak observed for each chondrule group. It should be noted that chondrules for which individual Pb–Pb ages have been reported are exceptionally large⁴⁷ and may, therefore, be unrepresentative of the broader chondrule population. The Pb–Pb ages may also be shifted towards older ages due to loss of short-lived ²²²Rn in the ²³⁸U–²⁰⁶Pb decay chain⁵. Thus, in spite of the ancient Pb–Pb ages reported for a few chondrules, there is little doubt that the vast majority of chondrules formed between ~2 and ~4 Myr after CAI formation.

Besides estimates based on chondrule ages, the accretion times of chondrite parent bodies have also been determined using

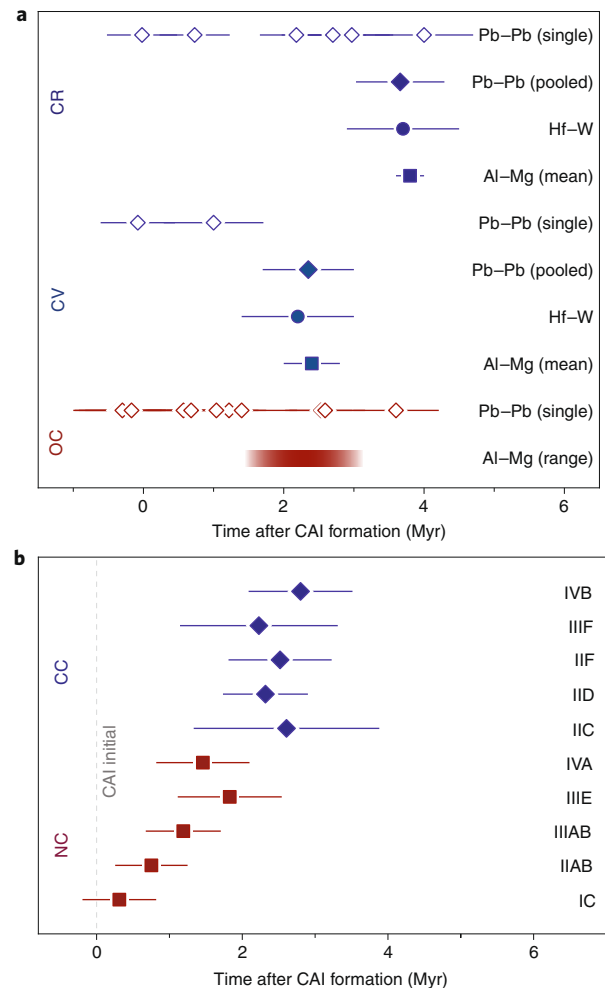


Fig. 3 | Summary of isotopic ages discussed in the text, shown as age intervals relative to CAI formation. a, Pb–Pb, Al–Mg and Hf–W ages of chondrules. Distinguished are Pb–Pb of single chondrules (open symbols; refs. ^{3,44}) and pooled chondrule separates (closed symbols; refs. ^{40–43}), Al–Mg ages of ordinary chondrite (OC) chondrules, CV chondrules and CR chondrules (refs. ^{5,36–39}), and Hf–W ages of CV and CR chondrules (refs. ^{29,34}). Note that absolute Pb–Pb ages were recalculated to age intervals for easy comparison, and all Pb–Pb ages shown are corrected for U isotope variability⁹⁰. **b**, Core formation of magmatic iron meteorites based on Hf–W chronometry^{4,9}. Distinguished are NC (IC, IIAB, IIIAB, IIIIE, IVA) and CC (IIC, IID, IIF, IIIIF, IVB) iron meteorite groups. Ages for CAIs and Solar System initial values are from refs. ^{3,19,30,54}.

thermal modelling of asteroids heated internally by ²⁶Al decay, combined with either the inferred peak metamorphic temperatures reached inside these bodies⁴⁹ or with the chronology of alteration products (for example, carbonates and secondary fayalites)^{50–52}. Using these approaches generally results in accretion ages that are consistent with the isotopic ages of chondrules. For instance, for the CV chondrite parent body, the 2.5–3.3 Myr accretion age obtained from thermal modelling^{50,51} is in good agreement with the aforementioned CV chondrule ages of 2–3 Myr after CAI formation. For CM chondrites, for which no chondrule ages are available, a 3.0–3.5 Myr accretion age is obtained⁵², suggesting that this body formed somewhat later than the ordinary, CV and CO chondrite parent bodies (Fig. 3a).

In summary, the chronology of chondrules and secondary alteration products in primitive chondrites, as well as thermal modelling

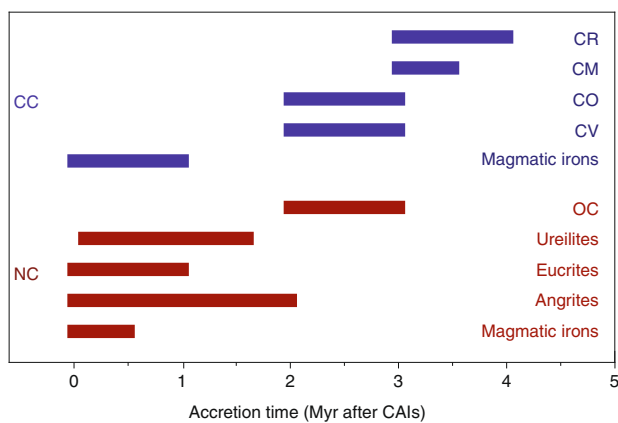


Fig. 4 | Accretion timescales of meteorite parent bodies as inferred from isotopic ages of meteorites. Accretion ages of iron meteorite, angrite and eucrite parent bodies are inferred from model ages for differentiation combined with thermal modelling for internal heating of the parent bodies by ^{26}Al decay (see text). Accretion timescales for chondrite parent bodies are based on Al–Mg, Hf–W and Pb–Pb ages obtained for chondrules, and on the chronology of alteration products combined with thermal modelling (see text). Note that the horizontal bars reflect the uncertainty of the accretion age estimates, and not the duration of accretion.

of bodies heated by ^{26}Al decay, indicate that chondrite parent-body accretion occurred between ~ 2 and ~ 4 Myr after CAI formation, and post-dated the accretion of differentiated asteroids. In the NC reservoir, meteorite parent-body accretion ceased at ~ 2 Myr, when the ordinary chondrite parent bodies formed, but in the CC reservoir continued until at least ~ 3 – 4 Myr, when the CR and CM chondrite parent bodies formed (Fig. 4).

Dynamical implications of the NC–CC dichotomy

Linking the chronology of meteorite parent-body accretion with the NC–CC dichotomy provides fundamentally new insights into the dynamics and large-scale structure of the solar protoplanetary disk, the formation and growth history of Jupiter, and the accretion dynamics of terrestrial planets, including the delivery of water and highly volatile species to Earth.

Origin of the dichotomy and structure of the solar protoplanetary disk.

To understand the origin of the NC–CC dichotomy, it is useful to summarize its three key characteristics. First, the dichotomy requires a larger fraction of nuclides produced in neutron-rich stellar environments to be present in the CC reservoir compared with the NC reservoir. This is manifest by enrichments in ^{50}Ti , ^{54}Cr , and r -process Mo isotopes in CC materials relative to NC materials. Second, the same isotopic characteristics, but with more pronounced enrichments, are typically also found in CAIs^{11,53}, which are known to have formed very early^{3,41,54,55}. Finally, the dichotomy exists for both refractory (for example, Ti, Mo) and non-refractory (for example, Cr, Ni) elements, which were probably hosted in distinct carriers. On the basis of these observations, two potential scenarios for the origin of the dichotomy can be ruled out. First, the dichotomy cannot reflect preferential destruction and volatilization of isotopically anomalous material from thermally labile presolar carriers by locally elevated temperatures within the disk, because such ‘thermal processing’ would have probably resulted in disparate effects on carriers of elements with different volatilities. Moreover, there is no a priori reason why thermal processing would solely affect carriers from specific neutron-rich stellar environments, and not also other carrier phases. Second, the dichotomy also cannot solely result from admixing of isotopically anomalous CAIs

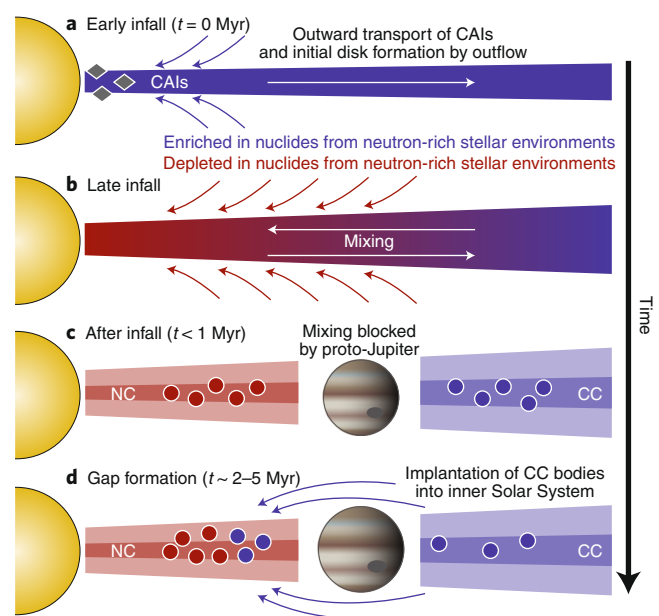


Fig. 5 | Evolution of the solar accretion disk. **a**, Rapid expansion of early infalling material by viscous spreading produces an initial disk, whose isotopic composition may be recorded in CAIs. **b**, Later infalling material was probably more depleted in neutron-rich isotopes (that is, NC-like). Mixing within the disk probably reduced the initial isotopic difference between solids from the inner and outer disk. **c**, The subsequent rapid formation of Jupiter’s core probably prevented exchange and mixing of disk materials, thereby maintaining an isotopic difference between the NC and CC reservoirs. **d**, Finally, the further growth of Jupiter resulted in the formation of a gap within the disk. This coincided with scattering of CC bodies from the outer disk into the main asteroid belt⁶⁶, either through Jupiter’s growth on a fixed orbit and/or by inward migration of Jupiter⁶⁷. Figure adapted with permission from ref. ¹³, Elsevier.

to the CC reservoir, because CAIs contain too little Cr and Ni to have a notable effect on the isotopic composition of these elements throughout the outer disk^{13,56}.

Instead, the key characteristics of the dichotomy outlined above are more readily explained if the isotopic difference between the NC and CC reservoirs is inherited from the Solar System’s parental molecular cloud and was imparted onto the protoplanetary disk during infall from the collapsing protostellar envelope (Fig. 5). For instance, in a model proposed by Nanne et al.¹³ and Burkhardt et al.⁵⁶, the isotopic composition of early-infalling material is characterized by enrichments in nuclides from neutron-rich stellar environments and is similar to that recorded in CAIs, which formed close to the Sun and were subsequently transported outwards by rapid viscous spreading of the disk^{57–59}. This earliest disk would have contained not only CAIs but also other, less refractory, dust particles⁵⁶. Later infalling NC material was depleted in nuclides from neutron-rich stellar environments, and provided most of the mass of the inner disk⁵⁹. The model assumes that the outer disk, which had formed by viscous spreading of early infalling material, extended beyond the radius at which the later infalling material is added (Fig. 5). In this case, a signature of the earliest disk would be preserved, in diluted form, as the composition of the CC reservoir, which is intermediate between those of early infalling (that is, CAI-like) and late-infalling (that is, NC-like) material. The strength of this model is that it readily accounts for the formation of CAIs close to the Sun, their subsequent outward transport and the isotopic link between CAIs and the CC reservoir by the same process, namely the rapid radial expansion of early-infalling material¹³. Finally, an origin of the

NC–CC dichotomy during later infall implies that the Solar System’s parental molecular cloud was isotopically heterogeneous. It is important to recognize that the magnitude of this isotopic heterogeneity is on the order of only ~0.1%. Such extremely small heterogeneities are not improbable in the large and dynamic structures of molecular clouds.

The Jupiter barrier. Linking the NC–CC dichotomy (‘The non-carbonaceous–carbonaceous meteorite dichotomy’) with the chronology of meteorite parent-body accretion (‘Meteorite chronology in light of the NC–CC dichotomy’) provides key constraints on the formation and growth history of Jupiter. In particular, the chronology of meteorites demonstrates that meteorite parent-body accretion in the NC and CC reservoirs commenced very early and continued concurrently for several million years in both reservoirs⁹ (Fig. 4). Importantly, the characteristic Mo isotope signatures of the NC and CC reservoirs did not change substantially during this period, as is evident from the observation that in each reservoir, early-formed iron meteorites and later-formed chondrites plot on single s-process mixing lines (that is, the NC and CC lines; Fig. 2a). The data allow for some deviations from each line, which may reflect small variations in the characteristic r-process signatures of the NC and CC reservoirs, but these differences are small compared with the overall offset between the NC and CC lines. Combined, these data indicate that the NC and CC reservoirs co-existed, and maintained their isotopic differences, for several million years⁹.

As is evident from the Hf–W ages for iron meteorites, planetesimal accretion in both the NC and CC reservoirs commenced very early. Consequently, one way to explain the characteristic NC–CC isotopic difference sampled by these objects is that it reflects the rapid accretion of dust into planetesimals with more stable orbits, hampering any further mixing of dust from the NC and CC reservoirs. However, this explanation cannot account for the observation that planetesimals with the same characteristic NC–CC isotopic difference (that is, the chondrite parent bodies in both reservoirs; Fig. 4) continued to accrete for several million years, because the rapid radial transport of dust in the disk^{60,61} would have homogenized the NC–CC isotopic difference on a much shorter timescale. The prolonged spatial separation of the NC and CC reservoirs, therefore, requires a barrier against radial transport of material. The most likely candidate for this barrier is the formation of Jupiter⁹, which would have inhibited the inward drift of most dust particles^{62,63}, preserving the distinct isotopic compositions of the NC and CC reservoirs. By blocking the sunward drift of dust, the Jupiter barrier also led to a mass-deficient inner Solar System, ultimately resulting in the Solar System’s bimodal structure of four smaller terrestrial planets surrounded by four gas giant planets⁶³.

In detail, the efficiency of the Jupiter barrier depends on the grain size of the dust drifting inwards, and on the size (and hence growth history) of Jupiter. For instance, the Jupiter barrier may have resulted in a strong filtering effect, whereby small dust grains could still pass through, whereas the drift of larger grains was efficiently prohibited⁶⁴. While this process may have resulted in small isotopic changes within the NC reservoir, it evidently did not lead to notable departures of meteorite compositions from the NC line¹⁸, either because the inward drifting CC dust was not accreted efficiently by NC parent bodies⁶⁵ or because the total mass of this material was not sufficient to substantially change the composition of the inner disk^{9,18}.

Not only does Jupiter provide the necessary barrier for separating the NC and CC reservoirs but its growth⁶⁶ and/or migration⁶⁷ also provide a mechanism for the inward scattering of CC bodies into the inner Solar System. This accounts for the co-occurrence of both types of bodies in the present-day asteroid belt, implying that the compositional diversity of main belt asteroids reflects their formation over a wide range of heliocentric distances. Furthermore,

the inward scattering of objects from beyond Jupiter’s orbit also provides a mechanism for the delivery of CC bodies to the growing terrestrial planets⁶⁶.

Growth history of Jupiter. The standard model for the formation of Jupiter is the core accretion model⁶⁸, in which Jupiter’s gaseous envelope is accreted onto a ‘solid’ core of 10–20 Earth masses (M_{\oplus}). Once Jupiter’s core reached ~20 M_{\oplus} it substantially hampered the inward drift of dust grains⁶², and when Jupiter reached ~50 M_{\oplus} it opened a gap in the disk⁶⁹, ultimately leading to inward migration⁶⁷ of Jupiter and gravitational scattering⁶⁶ of bodies from beyond its orbit into the inner Solar System (Fig. 5). Within the framework of this model for Jupiter’s formation, and under the assumption that the growth of Jupiter is responsible for the initial separation of the NC and CC reservoirs, the timescale of its growth can be estimated from the chronology of meteorite parent-body accretion within the NC and CC reservoirs.

The tightest constraint on the timescale of Jupiter’s growth is provided by the early accretion times of NC and CC iron meteorite parent bodies. As the characteristic r-process Mo isotopic difference between the NC and CC reservoirs did not change substantially after the first planetesimals (that is, the iron meteorite parent bodies) had formed in each reservoir, Jupiter’s core was likely grown to near its final size by the time the oldest NC planetesimals formed, at <0.5 Myr after CAI formation⁹. Such a rapid accretion of Jupiter’s core probably requires formation by pebble accretion^{68,70,71}.

Constraining Jupiter’s subsequent growth history is more difficult. In the simplest case, the accretion ages of NC and CC meteorites reflect the period of time over which no mixing between both reservoirs occurred⁹. In this case, dynamical mixing of NC and CC bodies could have only occurred after formation of the youngest CC bodies⁹ at ~3.7 Myr after CAI formation²⁹. In detail, however, the effect of Jupiter’s growth on the composition of the NC and CC reservoirs was probably more complicated. Accretion of CC bodies may still have occurred while Jupiter already scattered earlier-formed CC bodies into the inner Solar System, and so Jupiter may have reached ~50 M_{\oplus} earlier than ~3.7 Myr after CAI formation. For instance, within the framework of the Grand Tack model⁶⁷, Jupiter’s migration through the asteroid belt would have terminated planetesimal formation there, so in this case, Jupiter would have probably reached a mass of ~50 M_{\oplus} by ~2 Myr, the accretion age of the youngest NC meteorites (the ordinary chondrites). However, if Jupiter never migrated through the asteroid belt, then planetesimal formation in the NC reservoir may have also terminated through the depletion of gas inwards of Jupiter or because most of the dust had already been locked up in planetesimals. Nevertheless, so far there is no observational evidence suggesting inward scattering of CC bodies during the time of NC meteorite parent-body accretion, and so it seems unlikely that Jupiter reached ~50 M_{\oplus} before ~2 Myr. Note that the earliest observed influx of CC bodies into the inner Solar System is at ~4 Myr, as recorded in the H isotopic composition of eucrites and angrites^{72,73}. Consistent with this, angrites dated at ~4–5 Myr after CAI formation^{25,74} record the absence of a nebular magnetic field⁷⁵, indicating that by this time the nebular gas had dissipated. As Jupiter can only grow to its final size of ~318 M_{\oplus} in the presence of nebular gas, Jupiter’s accretion must have been completed by this time⁷⁵. Taking all these observations together suggests that Jupiter’s core of 10–20 M_{\oplus} accreted within <0.5 Myr, while Jupiter reached ~50 M_{\oplus} after ~2 Myr, and its final size of ~318 M_{\oplus} before ~4–5 Myr. This timescale of Jupiter’s accretion is consistent with predictions of the core accretion model^{68,76}.

Accretion of Earth. The NC–CC dichotomy provides a powerful tool to test different terrestrial planet accretion scenarios, which primarily differ in terms of the extent of radial mixing and the provenance of accreted material⁷⁷. Of particular interest is the amount

of CC material accreted by Earth (and other terrestrial planets), because this material derives from the most distant sources and therefore provides the tightest constraints on the extent of radial mixing during terrestrial planet formation. However, for most elements, the inferred amount of CC material in Earth is uncertain, because, owing to isotopic variations within the NC reservoir (Fig. 1), it depends on the assumed endmember isotopic compositions of Earth's building material¹⁸. This situation is different for Mo isotopes, because the amount of CC material accreted by Earth can be determined from the position of Earth's primitive mantle (or bulk silicate Earth (BSE)) among the NC and CC lines, irrespective of the position of Earth's building material on these lines¹⁸. That the BSE plots between the NC and CC lines (Fig. 2b), therefore, indicates that 30–60% of the BSE's Mo derives from the CC reservoir¹⁸. As a siderophile (metal-loving) element, the Mo in the BSE predominantly derives from the last 10–20% of accretion, because the Mo from earlier stages has been largely removed into Earth's core⁷⁸. Thus, while these data provide no information on whether Earth accreted CC material during earlier stages, they demonstrate that Earth accreted substantial amounts of CC material late in its growth history.

The last 10–20% of Earth's accretion was strongly influenced by the giant impact that led to the formation of the Moon⁷⁹, and by the late veneer — the material added to Earth's mantle after this impact. Budde et al.¹⁸ have shown that the BSE's Mo isotopic composition is best reproduced by either a CC composition of the Moon-forming impactor, or by mixed NC–CC compositions for the impactor and the late veneer. In both cases, the Moon-forming impactor contributed CC material to Earth, implying that this body either was a CC embryo from the outer Solar System, or that it accreted substantial amounts of CC material itself before collision with Earth. Either way, the late accretion of CC material to Earth probably also delivered water and highly volatile species to Earth^{80,81}, suggesting that Earth's habitability is strongly linked to the very late stages of its formation.

Open questions and future steps

The discovery of the NC–CC isotopic dichotomy has dramatically changed the way in which meteorites are used for constraining the dynamical evolution of the early Solar System and the nature of planet formation. Despite this success, several important questions remain. The efficiency of the Jupiter barrier for separating the NC and CC reservoirs should be better understood, and the isotopic evolution, if any, of the NC reservoir resulting from the potential inward drift of CC dust remains to be quantified, both in terms of spatial heterogeneity and temporal evolution. A related question is whether the inferred rapid formation of Jupiter's core by pebble accretion is compatible with the limited influx of material from the outer into the inner disk mandated by the preservation of an NC–CC isotopic difference.

Another important future step will be to combine the isotopic evidence for the provenance of accreted material derived from the NC–CC dichotomy with dynamical models of terrestrial planet formation. For instance, a scenario linking the late accretion of outer Solar System material by Earth to an orbital instability of the gas giant planets around the time of the Moon-forming impact^{18,82} remains to be tested. It will also be important to combine the isotopic and dynamical constraints with the known chronology of terrestrial planet formation. For instance, Schiller et al.⁶⁵ proposed that Earth accreted a large fraction (~40%) of CC-derived dust from the outer Solar System very early, within the lifetime of the protoplanetary disk (that is, within ~5 Myr after CAI formation). One implication of this model is that about half of the Earth's mass was accreted by this time. However, the ¹⁸²Hf–¹⁸²W chronology of core formation on Earth indicates that such a rapid accretion is only possible for a very high degree of core–mantle re-equilibration during each impact,

including the Moon-forming event^{83–85}. It is unknown, however, whether such high degrees of equilibration have been achieved⁸⁶.

Finally, Mars will have a key role in addressing some of these issues, because it probably accreted within the first 10 Myr of the Solar System^{87,88}. As such, Mars may have recorded the inward scattering of CC bodies during Jupiter's growth and/or migration but may have also accreted CC-derived dust that passed through the Jupiter barrier. However, the nature, timing and magnitude of the addition of CC material to Mars have yet to be investigated⁸⁹. Clearly, addressing all these questions will lead to major advances in understanding the early Solar System and the fundamental process of planet formation.

Received: 14 June 2019; Accepted: 29 October 2019;

Published online: 16 December 2019

References

1. Brogan, C. L. et al. The 2014 ALMA long baseline campaign: first results from high angular resolution observations toward the HL Tau region. *Astrophys. J. Lett.* **808**, L3 (2015).
2. Morbidelli, A., Lunine, J. I., O'Brien, D. P., Raymond, S. N. & Walsh, K. J. Building terrestrial planets. *Annu. Rev. Earth Planet. Sci.* **40**, 251–275 (2012).
3. Connelly, J. N. et al. The absolute chronology and thermal processing of solids in the solar protoplanetary disk. *Science* **338**, 651–655 (2012).
4. Kruijer, T. S. et al. Protracted core formation and rapid accretion of protoplanets. *Science* **344**, 1150–1154 (2014).
5. Pape, J., Mezger, K., Bouvier, A. S. & Baumgartner, L. P. Time and duration of chondrule formation: constraints from ²⁶Al–²⁶Mg ages of individual chondrules. *Geochim. Cosmochim. Acta* **244**, 416–436 (2019).
6. Budde, G. et al. Molybdenum isotopic evidence for the origin of chondrules and a distinct genetic heritage of carbonaceous and non-carbonaceous meteorites. *Earth Planet. Sci. Lett.* **454**, 293–303 (2016).
7. Van Kooten, E. M. M. E. et al. Isotopic evidence for primordial molecular cloud material in metal-rich carbonaceous chondrites. *Proc. Natl Acad. Sci. USA* **113**, 2011–2016 (2016).
8. Warren, P. H. Stable-isotopic anomalies and the accretionary assemblage of the Earth and Mars: a subordinate role for carbonaceous chondrites. *Earth Planet. Sci. Lett.* **311**, 93–100 (2011).
9. Kruijer, T. S., Burkhardt, C., Budde, G. & Kleine, T. Age of Jupiter inferred from the distinct genetics and formation times of meteorites. *Proc. Natl Acad. Sci. USA* **114**, 6712–6716 (2017).
10. Zinner, E. in *Treatise on Geochemistry* 2nd edn (eds Holland, H. D. & Turekian, K. K.) 181–213 (Elsevier, 2014).
11. Dauphas, N. & Schauble, E. A. Mass fractionation laws, mass-independent effect, and isotopic anomalies. *Ann. Rev. Earth Planet. Sci.* **44**, 709–783 (2016).
12. McKeegan, K. D. et al. The oxygen isotopic composition of the Sun inferred from captured solar wind. *Science* **332**, 1528–1532 (2011).
13. Nanne, J. A. M., Nimmo, F., Cuzzi, J. N. & Kleine, T. Origin of the non-carbonaceous–carbonaceous meteorite dichotomy. *Earth Planet. Sci. Lett.* **511**, 44–54 (2019).
14. Regelous, M., Elliott, T. & Coath, C. D. Nickel isotope heterogeneity in the early Solar System. *Earth Planet. Sci. Lett.* **272**, 330–338 (2008).
15. Poole, G. M., Rehkämper, M., Coles, B. J., Goldberg, T. & Smith, C. L. Nucleosynthetic molybdenum isotope anomalies in iron meteorites — new evidence for thermal processing of solar nebula material. *Earth Planet. Sci. Lett.* **473**, 215–226 (2017).
16. Worsham, E. A., Bermingham, K. R. & Walker, R. J. Characterizing cosmochemical materials with genetic affinities to the Earth: genetic and chronological diversity within the IAB iron meteorite complex. *Earth Planet. Sci. Lett.* **467**, 157–166 (2017).
17. Burkhardt, C. et al. Molybdenum isotope anomalies in meteorites: constraints on solar nebula evolution and origin of the Earth. *Earth Planet. Sci. Lett.* **312**, 390–400 (2011).
18. Budde, G., Burkhardt, C. & Kleine, T. Molybdenum isotopic evidence for the late accretion of outer Solar System material to Earth. *Nat. Astron.* **3**, 736–741 (2019).
19. Amelin, Y. et al. U–Pb chronology of the Solar System's oldest solids with variable ²³⁸U/²³⁵U. *Earth Planet. Sci. Lett.* **300**, 343–350 (2010).
20. Kleine, T. & Wadhwa, M. in *Planetesimals: Early Differentiation and Consequences for Planets Cambridge Planetary Science* (eds Weiss, B. P. & Elkins-Tanton, L. T.) 224–245 (Cambridge Univ. Press, 2017).
21. Hevey, P. J. & Sanders, I. S. A model for planetesimal meltdown by ²⁶Al and its implications for meteorite parent bodies. *Meteorit. Planet. Sci.* **41**, 95–106 (2006).

22. Scott, E. R. D. Chemical fractionation in iron meteorites and its interpretation. *Geochim. Cosmochim. Acta* **36**, 1205–1236 (1972).
23. Bottke, W. F., Nesvorniy, D., Grimm, R. E., Morbidelli, A. & O'Brien, D. P. Iron meteorites as remnants of planetesimals formed in the terrestrial planet region. *Nature* **439**, 821–824 (2006).
24. Bizzarro, M., Baker, J. A., Haack, H. & Lundgaard, K. L. Rapid timescales for accretion and melting of differentiated planetesimals inferred from ^{26}Al – ^{26}Mg chronometry. *Astrophys. J.* **632**, L41–L44 (2005).
25. Kleine, T., Hans, U., Irving, A. J. & Bourdon, B. Chronology of the angrite parent body and implications for core formation in protoplanets. *Geochim. Cosmochim. Acta* **84**, 186–203 (2012).
26. Touboul, M., Sprung, P., Aciego, S. M., Bourdon, B. & Kleine, T. Hf–W chronology of the eucrite parent body. *Geochim. Cosmochim. Acta* **156**, 106–121 (2015).
27. Schiller, M., Connelly, J. N., Glad, A. C., Mikouchi, T. & Bizzarro, M. Early accretion of protoplanets inferred from a reduced inner Solar System ^{26}Al inventory. *Earth Planet. Sci. Lett.* **420**, 45–54 (2015).
28. van Kooten, E. M. M. E., Schiller, M. & Bizzarro, M. Magnesium and chromium isotope evidence for initial melting by radioactive decay of ^{26}Al and late stage impact-melting of the ureilite parent body. *Geochim. Cosmochim. Acta* **208**, 1–23 (2017).
29. Budde, G., Kruijjer, T. S. & Kleine, T. Hf–W chronology of CR chondrites: implications for the timescales of chondrule formation and the distribution of ^{26}Al in the solar nebula. *Geochim. Cosmochim. Acta* **222**, 284–304 (2018).
30. Kruijjer, T. S., Kleine, T., Fischer-Godde, M., Burkhardt, C. & Wieler, R. Nucleosynthetic W isotope anomalies and the Hf–W chronometry of Ca–Al-rich inclusions. *Earth Planet. Sci. Lett.* **403**, 317–327 (2014).
31. Budde, G., Kruijjer, T. S., Fischer-Gödde, M., Irving, A. J. & Kleine, T. Planetesimal differentiation revealed by the Hf–W systematics of ureilites. *Earth Planet. Sci. Lett.* **430**, 316–325 (2015).
32. Krot, A. N., Connolly, H. C. Jr & Russell, S. S. (eds) *Chondrules: Records of Protoplanetary Disk Processes* (Cambridge Univ. Press, 2018).
33. Alexander, C. M. O., Grossman, J. N., Ebel, D. S. & Ciesla, F. J. The formation conditions of chondrules and chondrites. *Science* **320**, 1617–1619 (2008).
34. Budde, G., Kleine, T., Kruijjer, T. S., Burkhardt, C. & Metzler, K. Tungsten isotopic constraints on the age and origin of chondrules. *Proc. Natl Acad. Sci. USA* **113**, 2886–2891 (2016).
35. Johnson, B. C., Minton, D. A., Melosh, H. J. & Zuber, M. T. Impact jetting as the origin of chondrules. *Nature* **517**, 339–341 (2015).
36. Kita, N. T. & Ushikubo, T. Evolution of protoplanetary disk inferred from ^{26}Al chronology of individual chondrules. *Meteorit. Planet. Sci.* **47**, 1108–1119 (2012).
37. Nagashima, K., Krot, A. N. & Komatsu, M. ^{26}Al – ^{26}Mg systematics in chondrules from Kaba and Yamato 980145 CV3 carbonaceous chondrites. *Geochim. Cosmochim. Acta* **201**, 303–319 (2017).
38. Villeneuve, J., Chaussidon, M. & Libourel, G. Homogeneous distribution of Al-26 in the Solar System from the Mg isotopic composition of chondrules. *Science* **325**, 985–988 (2009).
39. Schrader, D. L. et al. Distribution of ^{26}Al in the CR chondrite chondrule-forming region of the protoplanetary disk. *Geochim. Cosmochim. Acta* **201**, 275–302 (2017).
40. Amelin, Y. & Krot, A. N. Pb isotopic ages of the Allende chondrules. *Meteorit. Planet. Sci.* **42**, 1321–1335 (2007).
41. Amelin, Y., Krot, A. N., Hutcheon, I. D. & Ulyanov, A. A. Lead isotopic ages of chondrules and calcium-aluminum-rich inclusions. *Science* **297**, 1678–1683 (2002).
42. Connelly, J., Amelin, Y., Krot, A. N. & Bizzarro, M. Chronology of the Solar System's oldest solids. *Astrophys. J.* **675**, L121–L124 (2008).
43. Connelly, J. N. & Bizzarro, M. Pb–Pb dating of chondrules from CV chondrites by progressive dissolution. *Chem. Geol.* **259**, 143–151 (2009).
44. Bollard, J., Connelly, J. N. & Bizzarro, M. Pb–Pb dating of individual chondrules from the CBa chondrite Gujba: assessment of the impact plume formation model. *Meteorit. Planet. Sci.* **50**, 1197–1216 (2015).
45. Krot, A. N., Amelin, Y., Cassen, P. & Meibom, A. Young chondrules in CB chondrites from a giant impact in the early Solar System. *Nature* **436**, 989–992 (2005).
46. Johnson, B. C., Walsh, K. J., Minton, D. A., Krot, A. N. & Levison, H. F. Timing of the formation and migration of giant planets as constrained by CB chondrites. *Sci. Adv.* **2**, e1601658 (2016).
47. Bollard, J. et al. Early formation of planetary building blocks inferred from Pb isotopic ages of chondrules. *Sci. Adv.* **3**, e1700407 (2017).
48. Bollard, J. et al. Combined U-corrected Pb–Pb dating and ^{26}Al – ^{26}Mg systematics of individual chondrules — evidence for a reduced initial abundance of ^{26}Al amongst inner Solar System chondrules. *Geochim. Cosmochim. Acta* **260**, 62–83 (2019).
49. Sugiura, N. & Fujiya, W. Correlated accretion ages and $\epsilon^{54}\text{Cr}$ of meteorite parent bodies and the evolution of the solar nebula. *Meteorit. Planet. Sci.* **49**, 772–787 (2014).
50. Doyle, P. M. et al. Early aqueous activity on the ordinary and carbonaceous chondrite parent bodies recorded by fayalite. *Nat. Commun.* **6**, 7444 (2015).
51. Jogo, K. et al. Mn–Cr ages and formation conditions of fayalite in CV3 carbonaceous chondrites: constraints on the accretion ages of chondritic asteroids. *Geochim. Cosmochim. Acta* **199**, 58–74 (2017).
52. Fujiya, W., Sugiura, N., Hotta, H., Ichimura, K. & Sano, Y. Evidence for the late formation of hydrous asteroids from young meteoritic carbonates. *Nat. Commun.* **3**, 627 (2012).
53. Brennecka, G. A., Borg, L. E. & Wadhwa, M. Evidence for supernova injection into the solar nebula and the decoupling of r-process nucleosynthesis. *Proc. Natl Acad. Sci. USA* **110**, 17241–17246 (2013).
54. Jacobsen, B. et al. ^{26}Al – ^{26}Mg and ^{207}Pb – ^{206}Pb systematics of Allende CAIs: canonical solar initial $^{26}\text{Al}/^{27}\text{Al}$ ratio reinstated. *Earth Planet. Sci. Lett.* **272**, 353–364 (2008).
55. MacPherson, G. J., Kita, N. T., Ushikubo, T., Bullock, E. S. & Davis, A. M. Well-resolved variations in the formation ages for Ca–Al-rich inclusions in the early Solar System. *Earth Planet. Sci. Lett.* **331–332**, 43–54 (2012).
56. Burkhardt, C., Dauphas, N., Hans, U., Bourdon, B. & Kleine, T. Elemental and isotopic variability in Solar System materials by mixing and processing of distinct molecular cloud reservoirs. *Geochim. Cosmochim. Acta* **261**, 145–170 (2019).
57. Desch, S. J., Kalyaan, A. & O'D. Alexander, C. M. The effect of Jupiter's formation on the distribution of refractory elements and inclusions in meteorites. *Astrophys. J. Suppl. Ser.* **238**, 11 (2018).
58. Pignatale, F. C., Charnoz, S., Chaussidon, M. & Jacquet, E. Making the planetary material diversity during the early assembling of the Solar System. *Astrophys. J. Lett.* **867**, L23 (2018).
59. Yang, L. & Ciesla, F. J. The effects of disk building on the distributions of refractory materials in the solar nebula. *Meteorit. Planet. Sci.* **47**, 99–119 (2012).
60. Birnstiel, T., Dullemond, C. P. & Pinilla, P. Lopsided dust rings in transition disks. *Astron. Astrophys.* **550**, L8 (2013).
61. Weidenschilling, S. J. Aerodynamics of solid bodies in the solar nebula. *Mon. Not. R. Astron. Soc.* **180**, 57–70 (1977).
62. Lambrechts, M., Johansen, A. & Morbidelli, A. Separating gas-giant and ice-giant planets by halting pebble accretion. *Astron. Astrophys.* **572**, A35 (2014).
63. Morbidelli, A. et al. Fossilized condensation lines in the Solar System protoplanetary disk. *Icarus* **267**, 368–376 (2016).
64. Weber, P., Benítez-Llambay, P., Gressel, O., Krapp, L. & Pessah, M. E. Characterizing the variable dust permeability of planet-induced gaps. *Astrophys. J.* **854**, 153 (2018).
65. Schiller, M., Bizzarro, M. & Fernandes, V. A. Isotopic evolution of the protoplanetary disk and the building blocks of Earth and the Moon. *Nature* **555**, 507–510 (2018).
66. Raymond, S. N. & Izidoro, A. Origin of water in the inner Solar System: planetesimals scattered inward during Jupiter and Saturn's rapid gas accretion. *Icarus* **297**, 134–148 (2017).
67. Walsh, K. J., Morbidelli, A., Raymond, S. N., O'Brien, D. P. & Mandell, A. M. A low mass for Mars from Jupiter's early gas-driven migration. *Nature* **475**, 206–209 (2011).
68. Pollack, J. B. et al. Formation of the giant planets by concurrent accretion of solids and gas. *Icarus* **124**, 62–85 (1996).
69. Crida, A., Morbidelli, A. & Masset, F. On the width and shape of gaps in protoplanetary disks. *Icarus* **181**, 587–604 (2006).
70. Lambrechts, M. & Johansen, A. Forming the cores of giant planets from the radial pebble flux in protoplanetary discs. *Astron. Astrophys.* **572**, A107 (2014).
71. Levison, H. F., Kretke, K. A. & Duncan, M. J. Growing the gas-giant planets by the gradual accumulation of pebbles. *Nature* **524**, 322–324 (2015).
72. Sarafian, A. R. et al. Angrite meteorites record the onset and flux of water to the inner Solar System. *Geochim. Cosmochim. Acta* **212**, 156–166 (2017).
73. Sarafian, A. R., Nielsen, S. G., Marschall, H. R., McCubbin, F. M. & Monteleone, B. D. Early accretion of water in the inner Solar System from a carbonaceous chondrite-like source. *Science* **346**, 623–626 (2014).
74. Amelin, Y. U–Pb ages of angrites. *Geochim. Cosmochim. Acta* **72**, 221–232 (2008).
75. Wang, H. et al. Lifetime of the solar nebula constrained by meteorite paleomagnetism. *Science* **355**, 623–627 (2017).
76. Alibert, Y. et al. The formation of Jupiter by hybrid pebble–planetesimal accretion. *Nat. Astron.* **2**, 873–877 (2018).
77. Fischer, R. A., Nimmo, F. & O'Brien, D. P. Radial mixing and Ru–Mo isotope systematics under different accretion scenarios. *Earth Planet. Sci. Lett.* **482**, 105–114 (2018).
78. Dauphas, N. The isotopic nature of the Earth's accreting material through time. *Nature* **541**, 521–524 (2017).
79. Canup, R. M. & Asphaug, E. Origin of the Moon in a giant impact near the end of the Earth's formation. *Nature* **412**, 708–712 (2001).
80. Alexander, C. M. O. D. et al. The provenances of asteroids, and their contributions to the volatile inventories of the terrestrial planets. *Science* **337**, 721–723 (2012).
81. Marty, B. The origins and concentrations of water, carbon, nitrogen and noble gases on Earth. *Earth Planet. Sci. Lett.* **313–314**, 56–66 (2012).

82. Nesvorný, D., Vokrouhlický, D., Bottke, W. F. & Levison, H. F. Evidence for very early migration of the Solar System planets from the Patroclus–Menoetius binary Jupiter Trojan. *Nat. Astron.* **2**, 878–882 (2018).
83. Kleine, T. et al. Hf–W chronology of the accretion and early evolution of asteroids and terrestrial planets. *Geochim. Cosmochim. Acta* **73**, 5150–5188 (2009).
84. Kleine, T. & Walker, R. J. Tungsten isotopes in planets. *Annu. Rev. Earth Planet. Sci.* **45**, 389–417 (2017).
85. Rudge, J. F., Kleine, T. & Bourdon, B. Broad bounds on Earth's accretion and core formation constrained by geochemical models. *Nat. Geosci.* **3**, 439–443 (2010).
86. Deguen, R., Landeau, M. & Olson, P. Turbulent metal-silicate mixing, fragmentation, and equilibration in magma oceans. *Earth Planet. Sci. Lett.* **391**, 274–287 (2014).
87. Dauphas, N. & Pourmand, A. Hf–W–Th evidence for rapid growth of Mars and its status as a planetary embryo. *Nature* **473**, 489–492 (2011).
88. Nimmo, F. & Kleine, T. How rapidly did Mars accrete? Uncertainties in the Hf–W timing of core formation. *Icarus* **191**, 497–504 (2007).
89. Brasser, R., Dauphas, N. & Mojzsis, S. J. Jupiter's influence on the building blocks of Mars and Earth. *Geophys. Res. Lett.* **45**, 5908–5917 (2018).
90. Brennecka, G. A. et al. $^{238}\text{U}/^{235}\text{U}$ variations in meteorites: extant ^{247}Cm and implications for Pb–Pb dating. *Science* **327**, 449–451 (2010).
91. MacPherson, G. J. in *Treatise on Geochemistry* (eds Holland, H. D. & Turekian, K. K.) 1–47 (Pergamon, 2007).
92. Burkhardt, C. et al. Hf–W mineral isochron for Ca, Al-rich inclusions: age of the Solar System and the timing of core formation in planetesimals. *Geochim. Cosmochim. Acta* **72**, 6177–6197 (2008).
93. Kööp, L. et al. A link between oxygen, calcium and titanium isotopes in ^{26}Al -poor hibonite-rich CAIs from Murchison and implications for the heterogeneity of dust reservoirs in the solar nebula. *Geochim. Cosmochim. Acta* **189**, 70–95 (2016).
94. Sahijpal, S. & Goswami, J. N. Refractory phases in primitive meteorites devoid of ^{26}Al and ^{41}Ca : representative samples of first Solar System solids? *Astrophys. J.* **509**, L137–L140 (1998).
95. Wood, J. A. Meteoritic evidence for the infall of large interstellar dust aggregates during the formation of the Solar System. *Astrophys. J.* **503**, L101–L104 (1998).

Acknowledgements

We are grateful to G. Budde and C. Burkhardt for many discussions about the NC–CC dichotomy, and for the collaborative effort that led to the identification of the dichotomy and for the development of some of the ideas presented in this Review. We thank G. Brennecka, J. Cuzzi, A. Morbidelli, F. Nimmo and E. A. Worsham for discussions. This study was performed under the auspices of the US DOE by Lawrence Livermore National Laboratory under contract DE-AC52-07NA2734. Funding from the Laboratory Directed Research and Development Program at Lawrence Livermore National Laboratory (grant 17-ERD-001 to L.E.B. and grant 20-ERD-001 to T.S.K.), from the European Research Council (ERC Consolidator grant number 616564 'ISOCORE' to T.K.) and from the Deutsche Forschungsgemeinschaft as part of the Collaborative Research Center TRR 170 (subproject B3) is gratefully acknowledged. This is TRR publication no. 81.

Competing interests

The authors declare no competing interests.

Additional information

Correspondence should be addressed to T.S.K.

Peer review information *Nature Astronomy* thanks Nathan Kaib and Edward Scott for their contribution to the peer review of this work.

Reprints and permissions information is available at www.nature.com/reprints.

Publisher's note Springer Nature remains neutral with regard to jurisdictional claims in published maps and institutional affiliations.

This is a U.S. government work and not under copyright protection in the U.S.; foreign copyright protection may apply 2019